

Time Modulation to Manage and Increase the Power Harvested From External Vibrations

Alireza Nikzamir*, Kasra Rouhi*, Alexander Figotin, and Filippo Capolino

Abstract—We investigate how a single resonator with a time-modulated component extracts power from an external ambient source. However, the collected power is largely dependent on the precise choice of the modulation signal frequency. We focus on the power absorbed from external vibration using a one degree-of-freedom mechanical resonator where the damper has a time-varying component. We show that time modulation can make a significant difference in the amount of harvested power, leading to more than 10 times enhancement with respect to an analogous system without time modulation. We also find that a narrow band pair of peak and dip in the spectrum of the absorbed power occurs because of the presence of an exceptional point of degeneracy (EPD). In this narrow frequency range, the delay between the damper modulating signal and the external vibrating signal largely affects the collected power. The high frequency-selectivity of EPD-induced power management could potentially be used in sensing and spectrometer applications.

Index Terms—Energy harvesting, Exceptional point of degeneracy (EPD), Mechanical system, Oscillator, Power collection, Time varying system

Energy harvesting has attracted considerable interest in recent years in electrical [1], [2], [3] and mechanical systems [4], [5], [6]. Energy harvesting technology offers a battery-less strategy by recovering energy from ambient sources such as vibrations, wind, light etc., and transform it into another form, such as electrical power. Applications include micro-electromechanical systems (MEMS) vibration energy harvesters [7], [8], low-power wireless sensors [9], fluid energy harvesting [10], and biomechanical energy harvesters [11]. In some of these applications, only a small fraction of energy needs to be extracted to power devices, and it is particularly important when devices are isolated. Therefore, collected power from a nearby ambient source can be used to power the circuits inside the device. Focusing on mechanical mechanisms, different vibration-based energy harvesting methods have been used recently [12], [13], [14], [15], [16], [17], though more work needs to be done on utilizing parametric excitation in time-varying systems for vibration energy harvesting. Furthermore, analogous principles could be used to manage the absorption of vibration or filter out particular vibration frequencies in mechanical systems [18].

In general, low vibration amplitudes cannot be efficiently collected. Therefore, various mechanical and electrical approaches have been developed to increase energy harvesting

Alireza Nikzamir, Kasra Rouhi, and Filippo Capolino are with the Department of Electrical Engineering and Computer Science, University of California, Irvine, CA 92697 USA, e-mails: anikzami@uci.edu, kasra.rouhi@uci.edu and f.capolino@uci.edu.

Alexander Figotin is with the Department of Mathematics, University of California, Irvine, CA 92697 USA, e-mail: afigotin@uci.edu.

* These authors contributed equally.

efficiency [19], [20], [21]. Vibration energy harvesters have been proposed with different nonlinear arrangements that increase their frequency range and dynamic range, most notably using nonlinear springs and dampers [22], [23]. Moreover, semi-active strategies and nonlinear damping in the form of cubic damping [15], [16] and nonlinear piezoelectric converters [24], [25] have been used to extend an energy harvester's dynamic range. In addition, there is a lot of work on analyzing systems where the mass changes over time [26], [27], [28]. However, challenges remain about maximizing the amount of energy harvested, and new ideas should be further explored.

In this letter, a resonator with a linear time-periodic (LTP) damper is considered for harvesting or managing energy from an outside source, focusing on a mechanical mass-spring-damper resonator subject to external vibration [4], as shown in Fig. 1. However, the physical principle here discussed is general and can also be applied to other systems as shown in the Appendix A. We demonstrate how parametric LTP modulation can boost the amplitude of motion, enabling a more efficient flow from the energy source to the harvesting system. By applying time variation to the system, power harvesting is improved by 10 times in a specific frequency range compared to the unmodulated system. Moreover, we observe extremely narrow spectral features in the spectrum of the harvested energy and we provide an explanation by resorting to the concept of exceptional points of degeneracy (EPD). Such degeneracy is a point in the parameter space of a resonating system at which multiple eigenmodes coalesce in both their eigenvalues and eigenvectors [29]. The presence of a nontrivial Jordan block in the Jordan canonical form of the system matrix describing the system's evolution shows the occurrence of EPD, as was demonstrated in [30], [31], [32]. The concept of EPD has been investigated in circuits with loss and/or gain under parity-time symmetry [33], [34], and also in spatially [35], [36] and temporally periodic structures [37], [38], [39]. Moreover, the degenerate eigenvalues of the system are exceptionally sensitive to any perturbations in system parameters [40]. The EPD-based principle has been proposed to achieve high sensitivity in various possible sensing scenarios, including optical microcavities [41], electron beam devices [42], electronic resonators [34], [43], [44], [45], and optomechanical mass sensors [46].

The kinetic energy harvesting mechanical scheme discussed in this letter is shown in Fig. 1. The system consists of a mass connected to a spring and a damper with an additional time-varying portion, and it is excited by external vibration represented by the imposed displacement $y_s(t)$ assumed to be monochromatic. Here, m is the mass, k is the spring stiffness

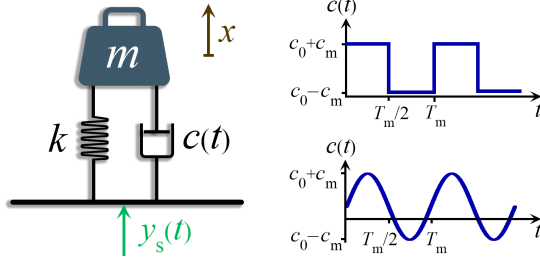


Fig. 1. Time-modulated mechanical system for kinetic energy harvesting. The external vibrational displacement of the whole system is $y_s(t)$. Two examples of time modulation of the damper are sinusoidal and two-level piece-wise constant (used in this paper).

constant, $c(t) = c_0 + c_m(t)$ is the damping parameter that includes a constant part c_0 and a time-periodic one $c_m(t)$ of period T_m (see right panel in Fig. 1). Also, x represents the mass displacement, and $y_s(t)$ is the imposed displacement of the system caused by an external force that drives the mechanical resonator. In addition, the electric counterpart circuit is shown in Appendix A. The governing equation of the time-varying system is

$$m\ddot{x} + c(t)(\dot{x} - \dot{y}_s) + k(x - y_s) = 0. \quad (1)$$

The constant damping coefficient $c_0 = c_p + c_t$ represents the energy losses within the system due to parasitic loss mechanisms c_p (e.g., viscous friction with air), and by the intentional mechanism of damping c_t , i.e., the mechanical energy extracted by the transduction mechanism [47], [48], [49]. Hence, part of the mobile mass's kinetic energy is lost in mechanical parasitic damping and some other is turned into electricity thanks to an energy converter (e.g., magnet/coil, piezoelectric material, variable capacitor, etc.) [50], [51], [52]. Here, we presume that the mechanical damping force is proportional to the velocity, which can be described as an electromechanical transducer [53, Ch. 2]. It is assumed that the mass of the vibration source is significantly greater than the mass m , so the external vibration is just modeled as an imposed force. We define the relative mass displacement parameter $z = x - y_s$, and the governing dynamic equation is rewritten as

$$\ddot{z} + 2\zeta(t)\omega_0\dot{z} + \omega_0^2 z = -\ddot{y}_s, \quad (2)$$

where $\zeta(t) = \zeta_0 + \zeta_m(t) = c_0/(2m\omega_0) + c_m(t)/(2m\omega_0)$ is the time-modulated damping rate and $\omega_0 = \sqrt{k/m}$ is the natural frequency of the unmodulated and lossless system. Assuming a time harmonic dependence of the form $z \propto e^{j\omega t}$ for the *unmodulated* homogeneous system (i.e., $c_m = 0$ and $y_s = 0$), we obtain the complex eigenfrequencies $\omega = \omega_0(\pm\sqrt{1 - \zeta_0^2} + j\zeta_0)$ associated to damped oscillations. To analyze the time-modulated system, we define the state vector as $\Psi(t) \equiv [z, \dot{z}]^T$, where the superscript T denotes the transpose operation, leading to

$$\begin{aligned} d\Psi(t)/dt &= \underline{\mathbf{M}}(t)\Psi(t) + \begin{pmatrix} 0 \\ -\ddot{y}_s \end{pmatrix}, \\ \underline{\mathbf{M}}(t) &= \begin{pmatrix} 0 & 1 \\ -\omega_0^2 & -2\zeta(t)\omega_0 \end{pmatrix}, \end{aligned} \quad (3)$$

where $\underline{\mathbf{M}}(t)$ is the time-variant system matrix. We first analyze the power transfer from an external monochromatic vibration $y_s(t) = y_0 \cos(2\pi f_s t)$, where y_0 is its amplitude and f_s is its frequency, into the LTP spring-mass-damper system using a time-domain numerical simulator (see Appendix A). We determine the time-averaged power P_s delivered by the external source $y_s(t)$, the time-averaged power P_m delivered by the time modulation, and the time-averaged power P_0 delivered to (or harvested by) the constant damper c_0 . Note that f_m is the modulation frequency of the time-varying damper, f_s is the frequency of the external source. In some designs, ambient vibrations are generally low in amplitude and frequency [51], so, we investigate how we can maximize both the power P_s absorbed from the external source and the power P_0 harvested by the constant damper by using time modulation.

A specific example is shown in Fig. 2, where $k = 4\pi^2 \text{ N/m}$ and $m = 1 \text{ kg}$ leading to $f_0 = 1 \text{ Hz}$, and $y_0 = 1 \text{ mm}$. We only consider for simplicity a two-level piece-wise constant time-periodic damping $c(t)$, which is equal to $c_0 + c_m$ in the time interval $0 \leq t < T_m/2$ and equal to $c_0 - c_m$ in $T_m/2 \leq t < T_m$. In this example, we assume $c_0 = 0.1 \text{ Ns/m}$ and $c_m = 0.15 \text{ Ns/m}$. We also study the unmodulated system with constant damper $c(t) = c_0$, where maximum energy can be extracted when the excitation frequency f_s matches the natural frequency of the system f_0 , as explained in Appendix B. In Fig. 2 we compare the LTP system with the unmodulated system to show that time modulation has a strong effect on the time-averaged power P_s absorbed from the source and on the power delivered to the constant portion of the damper P_0 . For the considered modulation frequency of $f_m = 2 \text{ Hz}$ that is equal to $2f_0$, P_s and P_0 are largely enhanced when f_s is in the neighbor of f_0 . The plot in Fig. 2(c) shows the maximum harvested power in the unmodulated system is $P_s = 19.7 \text{ mW}$, whereas the maximum power that the time modulated system absorbs from the source is $P_s = 198.4 \text{ mW}$, i.e., 10 times higher than that of the unmodulated system.

The results in Figs. 2(a)-(c) show also another interesting feature, i.e., the very narrow frequency range around $f_s = 0.992 \text{ Hz}$ where the power exhibits a sharp peak with abrupt changes when $f_m = f_{m,e}$, where $f_{m,e} = 1.984 \text{ Hz}$ is a modulation frequency that leads to the EPD, as shown next. This rapid power level variation is shown better in the zoomed-in frequency region in Figs. 2(d)-(f). The power level experiences a sharp maximum and a local minimum near $f_s = 0.992 \text{ Hz}$ (which is half of $f_{m,e}$). To understand the reasons for this very sharp peak and large variations in the time averaged power values we look at the eigenvalues of the system and their degeneracy.

To justify some of the above results, we look at the eigenstates of the time-varying system in the absence of an external vibration source, i.e., when $y_s = 0$. The evolution of the state

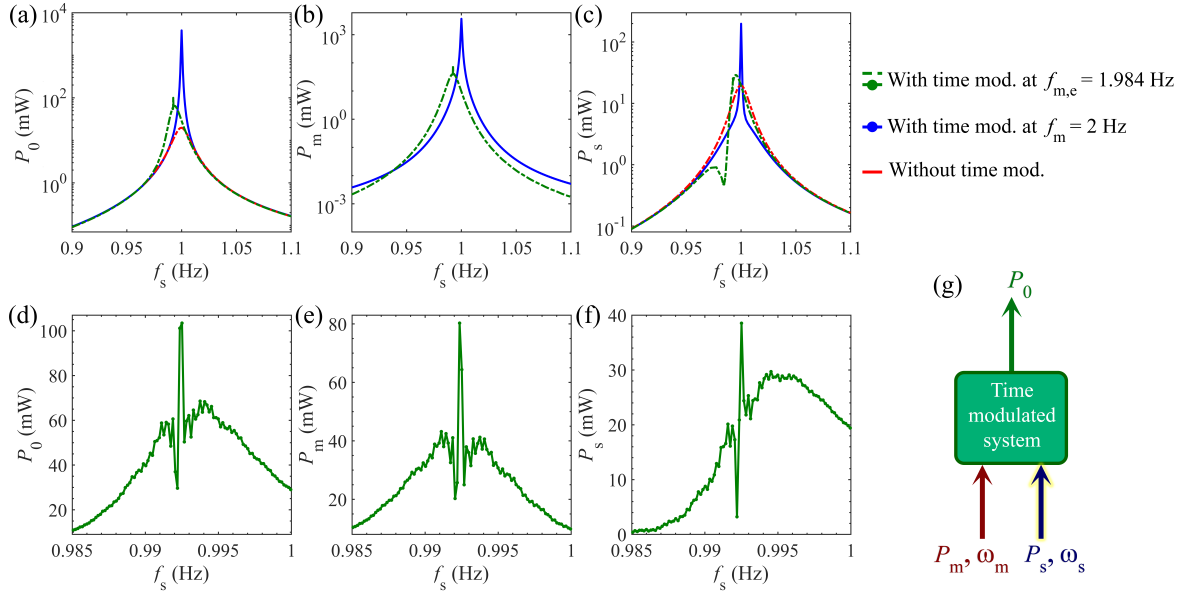


Fig. 2. Time-averaged power levels after reaching steady state for: (a) P_0 delivered to the damper c_0 ; (b) P_m provided by the time-varying damper $c_m(t)$; and (c) P_s extracted (harvested) from the external vibration, by varying the vibration frequency f_s in a wide range around $f_0 = 1$ Hz. Two time-modulated cases are considered here: modulation frequency $f_m = 2$ Hz at the center of the modulation gap (blue), and modulation frequency $f_m = f_{m,e} = 1.984$ Hz (green, note the sharp feature). For comparison, powers are also shown for the case without time modulation (red). (d)-(f) Zoomed-in analysis for frequencies near the EPD frequency $f_e = f_{m,e}/2 = 0.992$ Hz for the case with time modulation at $f_m = f_{m,e} = 1.984$ Hz. There is a remarkable highly varying power level around f_e . (g) Schematic of power diagram showing that the collected time-average power P_0 equals the sum of P_m and P_s .

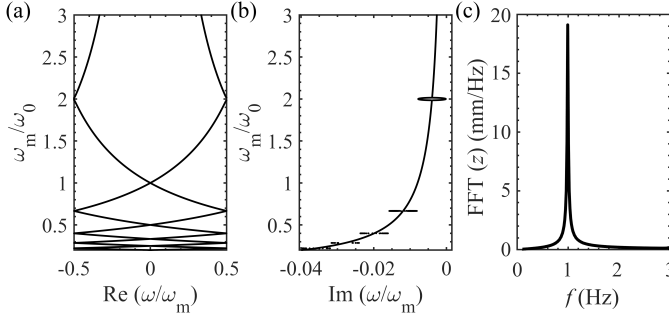


Fig. 3. The (a) real and (b) imaginary parts of eigenfrequencies $\omega + q\omega_m$, where q is an integer, of the system by varying ω_m . (c) Frequency spectrum of the relative mass displacement $z(t)$. The largest frequency spectral component of the displacement occurs at the fundamental harmonic $q = 0$, i.e., at the EPD frequency $f_e = f_{m,e}/2 = 0.992$ Hz.

vector in the LTP system with time periodicity T_m , from the time t to $t+T_m$, is given by $\Psi(t+T_m) = \Phi(t+T_m, t)\Psi(t)$, where $\Phi(t+T_m, t)$ is the state transition matrix, which is determined as $\Phi = e^{\underline{\mathbf{M}}_2 T_m/2} e^{\underline{\mathbf{M}}_1 T_m/2}$, where $\underline{\mathbf{M}}_1$ and $\underline{\mathbf{M}}_2$ are the system matrices in the first and second time intervals [54, Ch. 2]. We look for eigensolutions of the system that satisfy $\Psi(t+T_m) = e^{-j\omega T_m}\Psi(t)$ where ω (with all the harmonics $\omega + 2\pi q/T_m$, where q is an integer) is the complex eigenfrequency. Therefore, the eigenvalue problem is

$$\underline{\Phi}\Psi(t) = \lambda\Psi(t), \quad (4)$$

and the eigenvalues $\lambda_n = e^{-j\omega_n T_m}$, $n = 1, 2$, are obtained by solving the characteristic polynomial equation $\det(\underline{\Phi} - \lambda\mathbf{I}) = 0$. The eigensolutions $\Psi(t)$ have Fourier harmonics with frequencies $\omega_n + q\omega_m$, where $\omega_m = 2\pi f_m$,

is the modulation angular frequency [37]. When a transition matrix made of real values elements describes the system, the characteristic polynomial has real coefficients, so the eigenvalues are either real or complex conjugate pairs. The determinant of the transition matrix is written as [54, Ch. 2]

$$\det(\underline{\Phi}) = \lambda_1\lambda_2 = e^{[\text{tr}(\underline{\mathbf{M}}_1 T_m/2) + \text{tr}(\underline{\mathbf{M}}_2 T_m/2)]}, \quad (5)$$

where tr is the trace of the matrix. The determinant can be either $\det(\underline{\Phi}) = e^{2\text{Im}(\omega_1)T_m}$, when eigenvalues are complex conjugate pair, i.e., $\lambda_2 = \lambda_1^*$, or $\det(\underline{\Phi}) = e^{js\pi} e^{(\text{Im}(\omega_1) + \text{Im}(\omega_2))T_m}$, when λ_1 and λ_2 are both real and s is an integer. The two eigenvalues are

$$\lambda_{1,2} = \frac{\text{tr}(\underline{\Phi})}{2} \pm \sqrt{\left(\frac{\text{tr}(\underline{\Phi})}{2}\right)^2 - \det(\underline{\Phi})}, \quad (6)$$

and the two associated eigenvectors are

$$\Psi_1 = \begin{bmatrix} \varphi_{12} \\ \lambda_1 - \varphi_{11} \end{bmatrix}, \quad \Psi_2 = \begin{bmatrix} \varphi_{12} \\ \lambda_2 - \varphi_{11} \end{bmatrix}, \quad (7)$$

where φ_{11} and φ_{12} are elements of the matrix $\underline{\Phi}$. The two eigenvalues are degenerate ($\lambda_1 = \lambda_2 = \text{tr}(\underline{\Phi})/2$) when

$$\text{tr}(\underline{\Phi}) = \pm 2\sqrt{\det(\underline{\Phi})}. \quad (8)$$

According to Eq. (7), degenerate eigenvalues result in degenerate eigenvectors. At an EPD, the transition matrix is similar to a Jordan block with two degenerate eigenvalues $\lambda_1 = \lambda_2$ that are associated with degenerate eigenvectors. Thus, degenerate eigenvalues are sufficient to guarantee the degeneracy of the eigenvectors and hence the occurrence of an EPD. The formulation presented here is general and can be

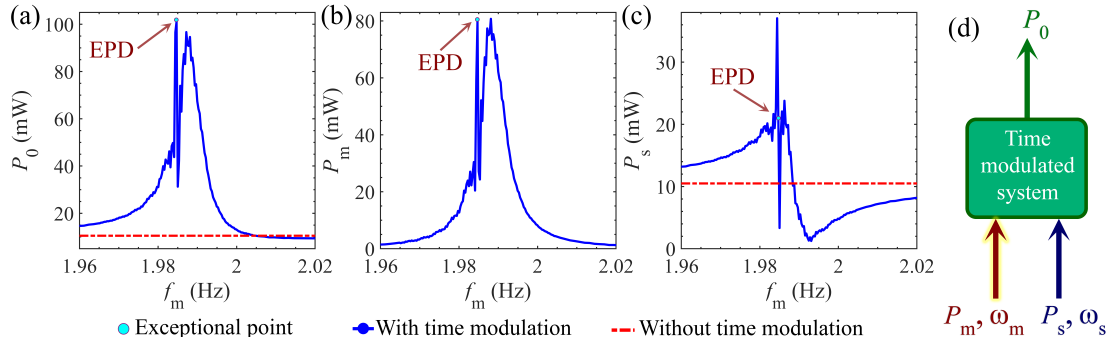


Fig. 4. Time-averaged powers by varying the modulation frequency f_m (blue curves), for the case of $f_s = f_{m,e}/2$. (a) P_0 delivered to the constant damper c_0 ; (b) P_m delivered by the time-varying damper $c_m(t)$; and (c) P_s collected from the source. The red dashed line is a reminder of the time-averaged power level of the unmodulated system. (d) Schematic of power diagram showing that the collected time-average power P_0 equals the sum of P_m and P_s .

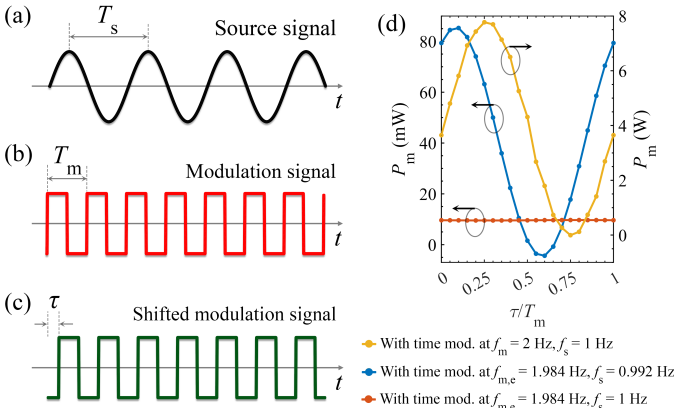


Fig. 5. (a) Source sinusoidal signal with a period of $T_s = 2T_m$. (b) Piece-wise constant time modulated damper with a period of T_m and (c) shifted by a delay τ . (d) Time-averaged power P_m delivered by the time-varying damper versus delay τ for three different scenarios. The value of P_m at EPD modulation frequency $f_{m,e} = 1.984$ Hz goes to a small value of $P_m = 0.04$ mW at the selected delay of $\tau/T_m = 0.51$.

applied to any system described by the differential equations of Eq. (3) in the absence of an external source term. As a matter of energy analysis, a time-periodic system is not isolated and it is continually interacting with the source of time-modulation. Therefore, energy can be transferred into or out of the system, i.e., the system can gain or lose energy from the time-variation source.

The eigenfrequency dispersion diagram of the mechanical system with the mentioned parameters is shown in Figs. 3(a) and (b). EPD happens at two modulated frequencies of $f_{m,e} = 1.984$ Hz and $f_{m,e} = 2.015$ Hz. Note that the quality factor of a resonating system is $Q = \text{Re}(\omega) / (2\text{Im}(\omega))$, which is higher for smaller $\text{Im}(\omega)$. Usually, a higher quality factor implies a higher power harvested by the system. A modulation gap in the dispersion diagram of eigenfrequencies happens when the two eigenfrequencies have two non-vanishing imaginary parts, i.e., between two closeby EPDs. When the modulation frequency is selected in the middle of the modulation gap, i.e., $f_m = 2$ Hz, one eigenfrequency has the smaller $\text{Im}(\omega)$, corresponding to a better quality factor compared to the two neighbor EPDs at slightly higher and lower frequencies. Thus, we expect the largest improvement in harvested power in the middle of the

modulation gap. Also, by selecting $f_{m,e} = 1.984$ Hz the system experiences harsh changes around $f_s = f_{m,e}/2 = 0.992$ Hz due to the degeneracy of the eigenfrequencies. The spectrum of the displacement $z(t)$ when the source-free system is modulated at $f_m = f_{m,e} = 1.984$ Hz and it is excited by an initial condition (see Appendix A for the calculation details) is illustrated in Fig. 3(c). The spectrum peak can be observed at $f_e = f_{m,e}/2 = 0.992$ Hz, that is same as the one obtained from solving the eigenvalue problem shown in Figs. 3(a) and (b).

When $f_m = f_{m,e} = 1.984$ Hz, the mechanical system operates at the EPD as shown in Figs. 3(a) and (b). The frequency domain spectrum in Fig. 3(c) shows that the first harmonic at $f = f_e = f_{m,e}/2 = 0.992$ Hz, carries the maximum power. After setting $f_s = f_e = f_{m,e}/2 = 0.992$ Hz, Figs. 4(a)-(c) show the powers by varying the modulation frequency around its EPD value $f_{m,e} = 1.984$ Hz. In this plot, time-modulated case is in blue curve, whereas the red dashed-line reminds the power values of the system without time-modulation. The numerical results show that the system operating very near to EPD (the EPD is the cyan point) harvests more power from the external source ($P_s = 20.9$ mW) compared to the system without time-modulation ($P_s = 10.5$ mW). Thus, time modulation leads to harvest more power from external vibration, with an improvement of 99%. In addition, the time-modulated element delivers the power of $P_m = 80.3$ mW to the system and the constant part of the damper absorbs $P_0 = P_s + P_m = 101.2$ mW from the system, at the EPD frequency.

The eigenfrequencies near the EPD are very sensitive to a system's variation, like a small change in the modulation frequency, as discussed in Appendix C. When such a small relative perturbation $\delta_m = (f_m - f_{m,e})/f_{m,e}$ is applied, the resulting two distinct eigenfrequencies $f_{1,2}(\delta_m)$ are estimated using the Puiseux series power expansion $f_{1,2}(\delta_m) \approx f_e \mp j(f_m/2\pi) \alpha_1 \sqrt{\delta_m}$ [39], where α_1 is the first-order coefficient of the series. The square root function demonstrates that the eigenfrequencies are highly sensitive to modulation frequency perturbations around the EPD, as shown in Fig. 3. This is reflected by the power levels that change dramatically when a small change in f_m is applied, as shown in Figs. 4(a)-(c). To harvest more power, the modulation frequency must be close to

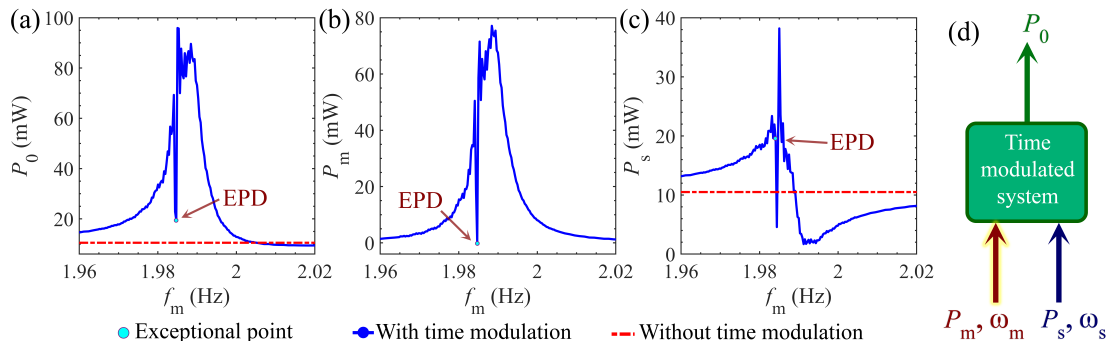


Fig. 6. Time-averaged power levels, after reaching steady state, as in Fig. 4, but assuming a time delay $\tau = 0.51T_m$ in the modulation of the damper, for the case of $f_s = f_{m,e}/2$.

the EPD frequency, but the modulation frequency value must also be precisely chosen.

To control the power provided by the time modulated portion of the circuit, Fig. 5(d) shows the time-averaged power P_m delivered by $c_m(t)$ versus delay, for $0 < \tau < T_m$. Three combinations of modulation and source frequencies are considered. For the two cases shown with blue and yellow curves in Fig. 5(d), we assume that the frequency of the source is fixed to $f_s = f_m/2$, hence, the period of the modulation signal is half of the source's one when operating at the EPD ($T_{m,e} = T_s/2$). In the third case (orange line), we assume that the modulation frequency is the EPD one, $f_m = f_{m,e}$, and source frequency at $f_s = 1$ Hz. It is clear that the variation of the delay τ has a strong effect on P_m when the modulation frequency is selected as $f_m = 2f_s$ (both blue and yellow curves). However, in the case shown by the orange curve, which is a slight modification from the other two cases, P_m is more or less constant and the delay does not have much effect on it. When $f_m = f_{m,e}$, and $f_s = f_m/2$ (blue curve), and at a specific delay $\tau = 0.51T_m$, the power delivered by the time-varying damper reaches the minimum and it is as small as $P_m = 0.04$ mW. By assuming the latter particular condition with $f_s = f_{m,e}/2$ and $\tau = 0.51T_m$, the numerical results in Fig. 6 show the source, modulation and constant damper powers by varying the modulation frequency (compared to the results in Fig. 4, where $\tau = 0$). Blue curves represent the power in the system with time modulation (note that the modulated power is near zero at the EPD), while red curves are the reminder of the power levels for the case without time modulation, as was done in Fig. 4. At the EPD modulation frequency $f_m = f_{m,e} = 1.984$ Hz (cyan point), the power extracted from the source vibration is $P_s = 19.38$ mW and the power delivered to the constant part of the damper c_0 is $P_0 = 19.42$ mW. Thus, time modulation improves power harvesting by 85% compared to the case without time modulation. Note also that in this case the power delivered by the modulation $P_m = 0.04$ mW is very small; so $P_0 \approx P_s$. However, the calculated powers around the EPD vary dramatically when changing the modulation frequency. That is one of the most peculiar properties associated with an EPD, as already depicted in Figs. 4, and 6. The reason is that the eigenstates at the EPD are extremely sensitive to any perturbation, as shown in Fig. 3, which causes a large degree of

variation when interacting with forced excitation. The system could possibly harvest even more power with a precise choice of modulation frequency close to EPD and proper time delay. However, even without a precise modulation frequency choice, the system harvests more power on average, over f_s or f_m variation.

As a conclusion, we have shown that a mechanical resonator with time modulation harvests much higher power (even ten times higher) from ambient vibration than its counterpart without time modulation. This effect can make a difference in applications where the ambient source amplitude is very low. Moreover, using the concept of second-order EPDs, we also explain the existence of a very sharp spectral peak at some modulation frequencies. The power levels vary rapidly with only a very slight variation in a parameter (like a modulation frequency) so great care must be taken when selecting the values of the modulation signal frequency. Indeed, using the Puiseux fractional series expansion, we have demonstrated that the degenerated system's eigenfrequency is highly sensitive to perturbations in the modulation frequency, and the physics associated with an EPD in an LTP mechanical system is vital to understand the EPD-related very narrow frequency feature of the power transfer mechanism. This effect could be exploited for sensing applications or for conceiving a very precise spectrometer.

ACKNOWLEDGMENTS

This material is based upon work supported by the Air Force Office of Scientific Research (AFOSR) under Grant No. FA9550-19-1-0103.

APPENDIX

A. Dual Circuit with Time-modulated Conductance

We show the analogous (dual) system made of a LC resonator and a linear time-periodic (LTP) conductance connected to the external source in series to the capacitor as shown in Fig. 7. In order to calculate the power in the dual LTP system, we consider piece-wise constant time-periodic conductance $G(t)$, i.e., $G(t) = G_0 + G_m$ during the time interval $0 \leq t < T_m/2$, and $G(t) = G_0 - G_m$ during the time interval $T_m/2 \leq t < T_m$. Analogously to the mechanical LTP system, we define the system state vector as $\Psi(t) = [v(t), \dot{v}(t)]^T$, where $v(t)$ is

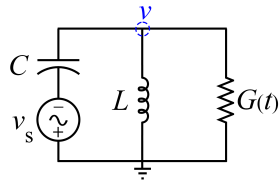


Fig. 7. The dual time-varying circuit where an inductance is connected in parallel to a time-varying conductance, with an external source $v_s(t)$ in series to the capacitor. The conductance is designed to have a two-level piece-wise constant time-periodic conductance, where $G(t) = G_0 + G_m$ during the time interval $0 \leq t < T_m/2$, and $G(t) = G_0 - G_m$ during the time interval $T_m/2 \leq t < T_m$.

the voltage on the inductor and $\dot{v}(t)$ is its time derivative. In general, $G(t)$ can be either lossy or gain (positive or negative respectively). Kirchhoff's circuit laws apply to time-varying circuits as follows:

$$G(t)\dot{v} + \frac{v}{L} + C(\ddot{v} + \ddot{v}_s) = 0. \quad (9)$$

The circuit equation is rewritten as

$$\ddot{v} + 2\alpha(t)\dot{v} + \omega_0^2 v = -\ddot{v}_s. \quad (10)$$

where $\alpha(t) = \alpha_0 + \alpha_m(t) = G_0/(2C) + G_m(t)/(2C)$ is the time-modulated damping factor and $\omega_0 = 1/\sqrt{LC}$ is the natural frequency of the unmodulated and lossless circuit. Assuming time harmonic dependence of the form $v \propto e^{j\omega t}$ for the unmodulated homogeneous circuit, we obtain the eigenfrequencies as $\omega = j\alpha(1 \pm \sqrt{1 - \omega_0^2/\alpha^2})$. By writing the differential equation in the eigenvalue problem format, the time evolution of the state vector $\Psi(t)$ is given by

$$\begin{aligned} d\Psi(t)/dt &= \underline{\mathbf{M}}_c(t)\Psi(t) + \begin{pmatrix} 0 \\ -\ddot{v}_s \end{pmatrix}, \\ \underline{\mathbf{M}}_c(t) &= \begin{pmatrix} 0 & 1 \\ -\omega_0^2 & -2\alpha(t) \end{pmatrix}, \end{aligned} \quad (11)$$

where $\underline{\mathbf{M}}_c(t)$ is the equivalent circuit matrix. The differential equation and the circuit matrix are dual to the time-varying mechanical system whose time-varying damper is connected to the spring and mass. The duality transformation is $k \rightarrow 1/L$, $m \rightarrow C$ and $c(t) \rightarrow G(t)$ and both systems have an external excitation $\dot{y}(t) \rightarrow \ddot{v}_s(t)$ as summarized in Table I [55]. Also, we show the duality of the characteristic equations in mechanical systems and their dual version in electric circuits in Table II. By applying the conversion between force and current ($\mathcal{F} \longleftrightarrow i$) and velocity and voltage ($\dot{z} \longleftrightarrow v$), Newton's equations and instantaneous mechanical power relate to the electric dual equations. We analyze the dual LTP circuit by using the Keysight Advanced Design System (ADS) time-domain simulator to calculate the power. We excite the circuit with a sinusoidal source at a frequency of f_s and the amplitude of 10 mV. Also, the capacitor has a 10 mV as an initial condition for the case where no external source excites the system. We numerically calculate the power using a built-in power block in the simulator and then report the time-averaged power based on 1000 time periods after the time domain signal saturates (i.e., for the time window from 3500 s to 4500 s).

B. Vibration Conversion

As already mentioned in the paper, $c_0 = c_p + c_t$ is responsible for the energy losses within the system due to parasitic loss mechanisms c_p (e.g., viscous friction with air), and by the intentional mechanism of damping c_t , i.e., the mechanical energy extracted by the transduction mechanism. This model is based on the idea that converting energy from an oscillating mass to electricity (whatever the mechanism is) can be modeled as a linear damper in a mass-spring system. This model is quite accurate for certain types of electromechanical converters, such as those analyzed by Williams and Yates [56]. For other types of converter, such as electrostatic and piezoelectric, the model may be modified. However, the conversion will always result in a loss of mechanical kinetic energy, which can be referred to as damping [57]. Despite the fact that the current damper model does not accurately model all kinds converter types, the present analysis can be extended to electrostatic and piezoelectric systems [57]. The power extracted from the mechanical system via c_t is due to electrically induced damping and it constitutes the whole time-averaged power P_0 if the parasitic damping vanishes. The instantaneous power in the constant part of the damper c_0 , i.e., the combination of parasitic loss mechanisms c_p and transduction mechanism c_t , can be calculated as a product of induced force $c_0\dot{z}$ and velocity \dot{z} . Thus, the absorbed instantaneous power in the constant part of the damper is expressed by

$$p_0(t) = c_0\dot{z}^2. \quad (12)$$

The total time-averaged power P_0 is calculated by averaging the time domain expression. In a monochromatic regime, assuming no modulation, the total time-averaged power dissipated within the damper, i.e., the power extracted via the transduction mechanism and the power lost by parasitic damping mechanisms, is given by [48], [53], [58]

$$P_0 = \frac{m\zeta_0\omega_0\omega_s^2 \left(\frac{\omega_s}{\omega_0}\right)^3 y_0^2}{\left(2\zeta_0\frac{\omega_s}{\omega_0}\right)^2 + \left(1 - \left(\frac{\omega_s}{\omega_0}\right)^2\right)^2}, \quad (13)$$

where y_0 is the magnitude of the source vibration, $\zeta_0 = \zeta_p + \zeta_t = c_0/(2m\omega_0)$ is the constant damping ratio. Maximum power dissipation within the generator occurs when the device is operated at $\omega_s = \omega_0$, and in this case the total time-averaged power dissipated in the constant part of the damper is given by

$$P_0 = \frac{m\omega_0^3 y_0^2}{4\zeta_0}. \quad (14)$$

C. Sensitivity to Perturbation

Sensitivity of a system's observable to a particular parameter is a measure of how much a perturbation to that parameter affects the observable quantity of the system. The eigenvalues of the system at exceptional points of degeneracy (EPDs) are extremely sensitive to parameter changes, which is a significant feature. Applying a perturbation to a system parameter

TABLE I
COMPONENT VALUES IN THE MECHANICAL SYSTEM AND THEIR DUAL VALUES IN THE DUAL ELECTRICAL CIRCUIT.

Mechanical system	Dual electrical circuit	Duality
$k = 4\pi^2 \text{ N/m}$	$L = 0.025 \text{ H}$	$k \rightarrow 1/L$
$m = 1 \text{ kg}$	$C = 1 \text{ F}$	$m \rightarrow C$
$c_0 = 0.1 \text{ Ns/m}$	$G_0 = 0.1 \text{ S}$	$c_0 \rightarrow G_0$
$c_m = 0.15 \text{ Ns/m}$	$G_m = 0.15 \text{ S}$	$c_m \rightarrow G_m$
$c(t) = \begin{cases} c_0 + c_m, & 0 \leq t < T_m/2 \\ c_0 - c_m, & T_m/2 \leq t < T_m \end{cases}$	$G(t) = \begin{cases} G_0 + G_m, & 0 \leq t < T_m/2 \\ G_0 - G_m, & T_m/2 \leq t < T_m \end{cases}$	$c(t) \rightarrow G(t)$

TABLE II
DUAL EQUATIONS IN THE MECHANICAL SYSTEM AND DUAL ELECTRICAL CIRCUIT, WHERE \mathcal{F} IS THE FORCE AND i IS THE CURRENT.

Mechanical system	Dual electrical circuit		
Spring	$\mathcal{F} = kz$	$i = (1/L) \int v dt'$	Inductor
Mass	$\mathcal{F} = m\ddot{z}$	$i = C\dot{v}$	Capacitor
Damper	$\mathcal{F} = c\dot{z}$	$i = Gv$	Conductance
Mechanical Power	$p = \mathcal{F}\dot{z}$	$p = iv$	Electrical Power
Duality			
$\mathcal{F} \longleftrightarrow i$			
$\dot{z} \longleftrightarrow v$			

such as the modulation frequency $\delta_m = (f_m - f_{m,e}) / f_{m,e}$, leads to a perturbed transition matrix $\underline{\Phi}(\delta_m)$ and perturbed eigenvalues $\lambda_p(\delta_m)$, with $p = 1, 2$. Therefore, the degenerate resonance frequency occurring at the EPD f_e , splits into two distinct resonance frequencies $f_p(\delta_m)$, due to a small perturbation δ_m . We can calculate the perturbed eigenvalues near the EPD by using the convergent Puiseux fractional power series expansion, with coefficients calculated using the explicit recursive formulas in [59]. In the presented mechanical system with a second-order EPD, we utilize a first-order approximation of the perturbed eigenvalues as

$$\lambda_p(\delta_m) \approx \lambda_e + (-1)^p \alpha_1 \sqrt{\delta_m}, \quad (15)$$

where λ_e is the eigenvalue at EPD and the first order coefficient is expressed by

$$\alpha_1 = \left(-\frac{\partial H(\delta_m, \lambda) / \partial \delta_m}{\frac{1}{2!} \partial^2 H(\delta_m, \lambda) / \partial \lambda^2} \right)^{\frac{1}{2}} \Big|_{\delta_m=0, \lambda=\lambda_e}, \quad (16)$$

where $H(\delta_m, \lambda) = \det(\underline{\Phi}(\delta_m) - \lambda \underline{I})$ and \underline{I} is the 2×2 identity matrix. The perturbed resonance frequencies are approximately calculated as

$$f_p(\delta_m) \approx f_e \pm j \frac{f_m}{2\pi} (-1)^p \alpha_1 \sqrt{\delta_m}. \quad (17)$$

This formula proves that the time-modulated system supporting the EPD is very sensitive to variations in the modulation frequency f_m . Figures 2, 4 and 6 of the paper demonstrate that the harvested power is very sensitive to variations in the system's parameters when operating at or near an EPD.

REFERENCES

- [1] S. Priya, "Modeling of electric energy harvesting using piezoelectric windmill," *Applied Physics Letters*, vol. 87, no. 18, p. 184101, 2005.
- [2] A. M. Wickenheiser and E. Garcia, "Power optimization of vibration energy harvesters utilizing passive and active circuits," *Journal of Intelligent Material Systems and Structures*, vol. 21, no. 13, pp. 1343–1361, 2010.
- [3] D. Motter, J. V. Lavarda, F. A. Dias, and S. d. Silva, "Vibration energy harvesting using piezoelectric transducer and non-controlled rectifiers circuits," *Journal of the Brazilian Society of Mechanical Sciences and Engineering*, vol. 34, pp. 378–385, 2012.
- [4] N. G. Stephen, "On energy harvesting from ambient vibration," *Journal of Sound and Vibration*, vol. 293, no. 1-2, pp. 409–425, 2006.
- [5] S. R. Anton and H. A. Sodano, "A review of power harvesting using piezoelectric materials (2003–2006)," *Smart Materials and Structures*, vol. 16, no. 3, p. R1, 2007.
- [6] I.-H. Kim, H.-J. Jung, B. M. Lee, and S.-J. Jang, "Broadband energy-harvesting using a two degree-of-freedom vibrating body," *Applied Physics Letters*, vol. 98, no. 21, p. 214102, 2011.
- [7] Y. Naito and K. Uenishi, "Electrostatic mems vibration energy harvesters inside of tire treads," *Sensors*, vol. 19, no. 4, p. 890, 2019.
- [8] H. Toshiyoshi, S. Ju, H. Honma, C.-H. Ji, and H. Fujita, "Mems vibrational energy harvesters," *Science and Technology of Advanced Materials*, vol. 20, no. 1, pp. 124–143, 2019.
- [9] J. A. Paradiso and T. Starner, "Energy scavenging for mobile and wireless electronics," *IEEE Pervasive computing*, vol. 4, no. 1, pp. 18–27, 2005.
- [10] S.-D. Kwon, "A t-shaped piezoelectric cantilever for fluid energy harvesting," *Applied Physics Letters*, vol. 97, no. 16, p. 164102, 2010.
- [11] Q. Li, V. Naing, and J. M. Donelan, "Development of a biomechanical energy harvester," *Journal of Neuroengineering and Rehabilitation*, vol. 6, no. 22, 2009.
- [12] A. Arrieta, P. Hagedorn, A. Erturk, and D. J. Inman, "A piezoelectric bistable plate for nonlinear broadband energy harvesting," *Applied Physics Letters*, vol. 97, no. 10, p. 104102, 2010.
- [13] S.-M. Jung and K.-S. Yun, "Energy-harvesting device with mechanical frequency-up conversion mechanism for increased power efficiency and wideband operation," *Applied Physics Letters*, vol. 96, no. 11, p. 111906, 2010.
- [14] M. Zilletti, S. J. Elliott, and E. Rustighi, "Optimisation of dynamic vibration absorbers to minimise kinetic energy and maximise internal power dissipation," *Journal of Sound and Vibration*, vol. 331, no. 18, pp. 4093–4100, 2012.
- [15] F. Di Monaco, M. G. Tehrani, S. J. Elliott, E. Bonisoli, and S. Tornincasa, "Energy harvesting using semi-active control," *Journal of Sound and Vibration*, vol. 332, no. 23, pp. 6033–6043, 2013.
- [16] M. G. Tehrani and S. J. Elliott, "Extending the dynamic range of an energy harvester using nonlinear damping," *Journal of Sound and Vibration*, vol. 333, no. 3, pp. 623–629, 2014.
- [17] M. Scapolan, M. G. Tehrani, and E. Bonisoli, "Energy harvesting using parametric resonant system due to time-varying damping," *Mechanical Systems and Signal Processing*, vol. 79, pp. 149–165, 2016.
- [18] W. Jiao and S. Gonella, "Intermodal and subwavelength energy trapping in nonlinear metamaterial waveguides," *Physical Review Applied*, vol. 10, no. 2, p. 024006, 2018.

- [19] D. Zhu, M. J. Tudor, and S. P. Beeby, "Strategies for increasing the operating frequency range of vibration energy harvesters: a review," *Measurement Science and Technology*, vol. 21, no. 2, p. 022001, 2009.
- [20] X. Tang and L. Zuo, "Enhanced vibration energy harvesting using dual-mass systems," *Journal of Sound and Vibration*, vol. 330, no. 21, pp. 5199–5209, 2011.
- [21] A. Bibo and M. Daqaq, "Investigation of concurrent energy harvesting from ambient vibrations and wind using a single piezoelectric generator," *Applied Physics Letters*, vol. 102, no. 24, p. 243904, 2013.
- [22] R. Ramlan, M. Brennan, B. Mace, and I. Kovacic, "Potential benefits of a non-linear stiffness in an energy harvesting device," *Nonlinear Dynamics*, vol. 59, no. 4, pp. 545–558, 2010.
- [23] H. Laalej, Z. Q. Lang, S. Daley, I. Zazas, S. Billings, and G. Tomlinson, "Application of non-linear damping to vibration isolation: an experimental study," *Nonlinear Dynamics*, vol. 69, pp. 409–421, 2012.
- [24] M. Ferrari, V. Ferrari, M. Guizzetti, B. Ando, S. Baglio, and C. Trigona, "Improved energy harvesting from wideband vibrations by nonlinear piezoelectric converters," *Sensors and Actuators A: Physical*, vol. 162, no. 2, pp. 425–431, 2010.
- [25] J. Cao, W. Wang, S. Zhou, D. J. Inman, and J. Lin, "Nonlinear time-varying potential bistable energy harvesting from human motion," *Applied Physics Letters*, vol. 107, no. 14, p. 143904, 2015.
- [26] W. Van Horssen, A. Abramian *et al.*, "On the free vibrations of an oscillator with a periodically time-varying mass," *Journal of Sound and Vibration*, vol. 298, no. 4–5, pp. 1166–1172, 2006.
- [27] W. Van Horssen, O. Pischansky, and J. Dubbeldam, "On the forced vibrations of an oscillator with a periodically time-varying mass," *Journal of Sound and Vibration*, vol. 329, no. 6, pp. 721–732, 2010.
- [28] M. Zukovic and I. Kovacic, "An insight into the behaviour of oscillators with a periodically piecewise-defined time-varying mass," *Communications in Nonlinear Science and Numerical Simulation*, vol. 42, pp. 187–203, 2017.
- [29] W. D. Heiss, "Exceptional points of non-Hermitian operators," *Journal of Physics A: Mathematical and General*, vol. 37, no. 6, pp. 2455–2464, Jan 2004.
- [30] M. I. Vishik and L. A. Lyusternik, "The solution of some perturbation problems for matrices and selfadjoint or non-selfadjoint differential equations i," *Russian Mathematical Surveys*, vol. 15, no. 3, pp. 1–73, 1960.
- [31] A. P. Seyranian, "Sensitivity analysis of multiple eigenvalues*," *Mechanics of Structures and Machines*, vol. 21, no. 2, pp. 261–284, 1993.
- [32] A. Figotin and I. Vitebskiy, "Oblique frozen modes in periodic layered media," *Physical Review E*, vol. 68, no. 3, p. 036609, Sep 2003.
- [33] T. Stehmann, W. Heiss, and F. Scholtz, "Observation of exceptional points in electronic circuits," *Journal of Physics A: Mathematical and General*, vol. 37, no. 31, pp. 7813–7819, 2004.
- [34] J. Schindler, A. Li, M. C. Zheng, F. M. Ellis, and T. Kottos, "Experimental study of active LRC circuits with PT symmetries," *Physical Review A*, vol. 84, no. 4, p. 040101, Oct 2011.
- [35] M. Y. Nada, M. A. Othman, and F. Capolino, "Theory of coupled resonator optical waveguides exhibiting high-order exceptional points of degeneracy," *Physical Review B*, vol. 96, no. 18, p. 184304, 2017.
- [36] A. F. Abdelshafy, M. A. Othman, D. Oshmarin, A. T. Almutawa, and F. Capolino, "Exceptional points of degeneracy in periodic coupled waveguides and the interplay of gain and radiation loss: Theoretical and experimental demonstration," *IEEE Transactions on Antennas and Propagation*, vol. 67, no. 11, pp. 6909–6923, 2019.
- [37] H. Kazemi, M. Y. Nada, T. Mealy, A. F. Abdelshafy, and F. Capolino, "Exceptional points of degeneracy induced by linear time-periodic variation," *Physical Review Applied*, vol. 11, no. 1, p. 014007, 2019.
- [38] K. Rouhi, H. Kazemi, A. Figotin, and F. Capolino, "Exceptional points of degeneracy directly induced by space-time modulation of a single transmission line," *IEEE Antennas and Wireless Propagation Letters*, vol. 19, no. 11, pp. 1906–1910, 2020.
- [39] H. Kazemi, M. Y. Nada, A. Nikzamir, F. Maddaleno, and F. Capolino, "Experimental demonstration of exceptional points of degeneracy in linear time periodic systems and exceptional sensitivity," *Journal of Applied Physics*, vol. 131, no. 14, p. 144502, 2022.
- [40] T. Kato, *Perturbation Theory for Linear Operators*, 1st ed. Springer Berlin, Heidelberg, 1966.
- [41] H. Hodaei, A. U. Hassan, S. Wittek, H. Garcia-Gracia, R. El-Ganainy, D. N. Christodoulides, and M. Khajavikhan, "Enhanced sensitivity at higher-order exceptional points," *Nature*, vol. 548, no. 7666, pp. 187–191, 2017.
- [42] K. Rouhi, R. Marosi, T. Mealy, A. F. Abdelshafy, A. Figotin, and F. Capolino, "Exceptional degeneracies in traveling wave tubes with dispersive slow-wave structure including space-charge effect," *Applied Physics Letters*, vol. 118, no. 26, p. 263506, 2021.
- [43] P.-Y. Chen, M. Sakhdari, M. Hajizadegan, Q. Cui, M. M.-C. Cheng, R. El-Ganainy, and A. Alu, "Generalized parity-time symmetry condition for enhanced sensor telemetry," *Nature Electronics*, vol. 1, no. 5, pp. 297–304, 2018.
- [44] K. Rouhi, A. Nikzamir, A. Figotin, and F. Capolino, "Exceptional point in a degenerate system made of a gyrator and two unstable resonators," *Physical Review A*, vol. 105, no. 3, p. 032214, 2022.
- [45] A. Nikzamir and F. Capolino, "Highly sensitive coupled oscillator based on an exceptional point of degeneracy and nonlinearity," *Physical Review Applied*, vol. 18, no. 5, p. 054059, 2022.
- [46] P. Djorwe, Y. Pennec, and B. Djafari-Rouhani, "Exceptional point enhances sensitivity of optomechanical mass sensors," *Physical Review Applied*, vol. 12, no. 2, p. 024002, 2019.
- [47] S. Beeby, M. Tudor, and N. White, "Energy harvesting vibration sources for microsystems applications," *Measurement Science and Technology*, vol. 17, no. 12, pp. R175–R195, 2006.
- [48] S. P. Beeby, R. N. Torah, M. J. Tudor, P. Glynne-Jones, T. O'Donnell, C. R. Saha, and S. Roy, "A micro electromagnetic generator for vibration energy harvesting," *Journal of Micromechanics and Microengineering*, vol. 17, no. 7, pp. 1257–1265, 2007.
- [49] S. Kundu and H. B. Nemade, "Modeling and simulation of a piezoelectric vibration energy harvester," *Procedia Engineering*, vol. 144, pp. 568–575, 2016.
- [50] A. Erturk, J. Hoffmann, and D. J. Inman, "A piezomagnetoelastic structure for broadband vibration energy harvesting," *Applied Physics Letters*, vol. 94, no. 25, p. 254102, 2009.
- [51] S. Boisseau, G. Despesse, and B. A. Seddik, "Nonlinear h-shaped springs to improve efficiency of vibration energy harvesters," *Journal of Applied Mechanics*, vol. 80, no. 6, p. 061013, 2013.
- [52] P. Basset, E. Blokhina, and D. Galayko, *Electrostatic kinetic energy harvesting*. John Wiley & Sons, 2016.
- [53] P. Spies, M. Pollak, and L. Mateu, *Handbook of energy harvesting power supplies and applications*. CRC Press, 2015.
- [54] J. A. Richards, *Analysis of periodically time-varying systems*. Springer Science & Business Media, 1983.
- [55] P. Le Corbeiller and Y.-W. Yeung, "Duality in mechanics," *The Journal of the Acoustical Society of America*, vol. 24, no. 6, pp. 643–648, 1952.
- [56] C. Williams and R. B. Yates, "Analysis of a micro-electric generator for microsystems," *sensors and actuators A: Physical*, vol. 52, no. 1–3, pp. 8–11, 1996.
- [57] S. Roundy, P. K. Wright, and J. Rabaey, "A study of low level vibrations as a power source for wireless sensor nodes," *Computer communications*, vol. 26, no. 11, pp. 1131–1144, 2003.
- [58] C. Wei and X. Jing, "A comprehensive review on vibration energy harvesting: Modelling and realization," *Renewable and Sustainable Energy Reviews*, vol. 74, pp. 1–18, 2017.
- [59] A. Welters, "On explicit recursive formulas in the spectral perturbation analysis of a Jordan block," *SIAM journal on matrix analysis and applications*, vol. 32, no. 1, pp. 1–22, 2011.